JOURNAL OF Materials CHEMISTRY

Interface characterisation and wettability properties of carbon particle reinforced copper alloy

J. F. Silvain,*[a] D. Coupard,[b] Y. Le Petitcorps,[a] M. Lahaye,[a] M. Onillon[a] and X. Goni[c]

[a]*ICMCB CNRS, Chateau Brivaza, Av. A. Schweitzer, F-33608 Pessac, France. E-mail: silvain@icmcb.u-bordeaux.fr*
[b]*ENSAM, Esplanade des Arts et Metiers, F-33405 Talence, France*
[c]*INASMET, Camino de Portuetxe 12, Bo de Igara, E-20009 San Sebastian, Spain*

Received 15th May 2000, Accepted 27th June 2000
Published on the Web 10th August 2000

The effect of carbide alloying elements such as chromium and tin upon the bonding state and the interfacial carbon/copper zone in a copper melt have been investigated. The reactivity behaviour, contact angle and the kinetics of wettability have been investigated for each system studied (C/Cu, C/Cu–Sn, C/Cu–Cr and C/Cu–Sn–Cr) using Auger electron spectroscopy and line profile/sessile drop experiments performed under ultra high vacuum conditions. Non-wetting systems such as C/Cu and C/Cu–Sn are characterised by (i) an adhesive solid–solid bond strength and van der Waals interactions and (ii) monotonous behaviour during experiments where the kinetics are controlled by the viscous flow of the liquid drop over the solid substrate. Wetting systems such as C/Cu–Cr and C/Cu–Sn–Cr show a completely different behaviour. For these two systems, chromium tends to segregate at the reinforcement/metal interface, forming a stable carbide compound. Chromium segregation and carbide formation processes lead to different kinetics of wettability which can be summarised in a three step process.

1. Introduction

Carbon particle reinforced copper matrix composites with a low thermal expansion coefficient, a good electric and thermal conductivity together with good wear and frictional characteristics, may be applied as mechanical bearing and spot welding electrode materials.[1,2] However, one difficulty in using graphite particles with copper is the lack of adhesion between the copper and graphite surfaces.[3] The mechanical and physical properties of such composites are strongly influenced by the interfacial zone between the particle and the matrix. Factors such as the thickness, morphology and composition of the interfacial zone can modify the load transfer characteristics of the composite or, in extreme cases, even damage one of the constituents of the composite.

Three main types of particle/matrix (P/M) interface may appear in metal matrix composites:

(1) The composite constituents are chemically stable, resulting in a sharp P/M interface where the load is physically transferred *via* a clamping effect due to the radial compressive stresses of the matrix against the particle. Usually the coefficient of thermal expansion (CTE) of the metal matrix is higher than that of the particle.

(2) Chemical instability between the constituents of the composite gives rise to the growth of a diffusion-controlled reaction zone, which results in an intermediate interface. Properties like thickness, toughness, and strain to rupture, may weaken the final composite characteristics.

(3) The interface chemistry is a combination of (1) and (2), resulting from diffusion[4] due to a difference in chemical potentials between the two phases. In this case, if the formation of an interface is absent, the continuity between the two phases (particle and matrix) is monotonous which will enhance the load transfer across the two phases of the composite.

Fortunately, the structure and properties of the interface between the reinforcement and the matrix can be adjusted efficiently by modifications of the reinforcements and/or of the matrix.[5] In the early 1970s, Arthur and Cho[6] showed the interaction between copper atoms and the graphite basal plane to be no more than a van der Waals force. Mortimer and Nicholas'[7] investigation led to an improvement in copper bonding to graphite and vitreous carbon by alloying copper with small amounts of an active metal. In the latter case, the active metal additions were intended to segregate to the interface and produce carbide, leading to improvements in copper wettability and adhesion to the reactive layer.

The present paper aims at investigating the effect of the addition of alloying elements to the metal melt on the bonding state and the reaction zone at the P/M interface. In order to study the interfacial reactions at the Cu, Cu10Sn, Cu1Cr, and Cu10Sn1Cr carbon interfaces and the kinetics of wettability of these systems, Cu-alloy/C composites were manufactured. The kinetics of wetting was studied by conventional sessile drop experiments where the alloying matrix is prepared *in situ* inside an ultra high vacuum chamber. The compositions and the nature of the phases formed at the interfaces under this controlled atmosphere were investigated by Auger electron spectroscopy (AES) line profile. AES is a well-established surface analysis technique where the quantification and chemistry of the interface can be determined. However, in order to improve the analysis and the interpretation of the data, a non-linear least squares fitting (NLLSF) technique was used.[8]

2. Experimental

2.1 Choice of additive element

As previously reported in the literature (see Table 1), the problem of poor wettability and work of adhesion is predominant in the carbon reinforced copper system. The aim of this study is to improve and control wettability. Two main methods can be used for this purpose. The first deals with

Table 1 Wettability results obtained for pure copper/carbon systems

Carbon substrate	Grade of graphitisation	Working atmosphere	T/K	θ/°	Reference
Vitreous carbon $R_a<0.1$ μm	0	$\leqslant 7\times10^{-3}$ Pa	1423	145	9
Vitreous carbon $R_a<0.01$ μm	0	10^{-4} Pa	1423	145	10
Polished polycrystalline graphite	97	$\leqslant 7\times10^{-3}$ Pa	1423	135	7
Polished polycrystalline graphite	97	10^{-3} Pa	1373	140	11
Polished polycrystalline graphite	97	10^{-5} Pa argon	1406	157	12
Pyrocarbon 2000 $R_a=200$ nm	15	10^{-2} Pa helium	1423	135±8	13
Vitreous carbon $R_a=2$ nm	0	10^{-2} Pa helium	1423	137±5	This work

increasing the wettability either by chemical treatment[14] or by inorganic coating[15] of the carbon surface, and the second by adding to the liquid metal an element that has a high affinity for carbon.

Since liquid metals almost always wet solid metal, a large choice of coating metals can be investigated. The coating of long carbon fibres with nickel and iron[16] has been proven to increase the interfacial strength of copper–carbon composites. However, because of the high cost of such electrochemical treatment and the difficulty involved in coating micron sized particles, this approach was rejected.

In agreement with the second possible choice for improving the wettability of the graphite surface, a chromium based copper matrix was chosen as a result of theoretical calculations and experiments performed previously.[17] The two matrices used are the pure Cu matrix and the Cu–10 wt%Sn matrix. The amount of chromium additive was fixed to 1 wt%.

2.2 Fabrication of the composite

Reactivity experiments. The composites were fabricated using a conventional squeeze casting process. The carbon preforms ($T_{preform}=350$ °C) were infiltrated by molten copper or a copper alloy matrix ($T_{matrix}=800$ °C). The pressures applied to the system were up to 100 MPa during the solidification step.

Simple carbon rods were also used to elaborate reactive samples. In this method, the carbon rod was incorporated inside the liquid metal under controlled conditions.

Because AES interfacial studies reported exactly similar reaction zones for each elaboration processes, the second experimental device was mainly used for studying the reactivity.

Wettability experiments. In order to avoid any oxidation artefacts, the copper alloys were prepared *in situ*, inside the chamber of the sessile drop experiment. For this purpose, the suitable alloying elements were set on top of a copper sample in order to prepare each binary or ternary alloy. The temperature was gradually increased to allow the additive element to diffuse within the copper sample, thus obtaining uniform chemical composition within the sample. In all cases, the metals used had a very low impurity content (less than 0.005 wt%).

2.3 Characterisation of the composite

AES experiments. The AES line profile data were acquired on a MICROLAB 310-F scanning Auger microprobe. The analysis conditions chosen were a voltage and beam current of 10 keV and 1 nA, respectively. The regions of interest for the analysis were oxygen (490–525 eV), aluminium (1375–1415 eV), carbon (260–300 eV), tin (420–440 eV), chromium (510–540 eV), and copper (900–940 eV). The data were taken in the conventional E N(E) mode.

Non-linear least squares fitting (NLLSF) analysis of this data was required to differentiate the possible chemical states of carbon (C–C, C–Cr), oxygen (contamination, O–Cr, O–Cu) and copper (Cu–Cu, Cu–O). The Eclipse data used on the VG MICROLAB 310-F uses a NLLSF routine developed from the methodology discussed by Ja Ber *et al.*[18]

Wettability experiments. *Concept considerations.* The wetting approached used in this study is based on the sessile drop technique: a liquid drop rests on a horizontal plane substrate where it equilibrates. In order to study the kinetics of wettability (states before equilibrium), the flowing behaviour of the liquid drop is continuously observed. The recording of the liquid drop's shape allows the drawing of the tangents of the profile on both (l: left, and r: right) sides of the drop. It is thus possible to measure the θ_r and θ_F contact angles, the width of the drop (d) and its height (h). When the mass of the drop is less than 100 mg, which applies to the present situation, the effect due to gravity is minimised and the drop may be considered as a segment of a sphere (see Fig. 1).

The θ contact angle, and both the width and height of the drop are related according to the following equation:

$$\theta = 2\ \arctan(2h/d)$$

At thermodynamic equilibrium, the contact angle θ formed by a liquid over an ideal solid substrate is related to the interfacial energies γ_{sv}, γ_{lv}, and γ_{sl}, which are respectively associated with the solid–vapour (sv), liquid–vapour (lv), and solid–liquid (sl) interfaces, by the Young's equation:[13]

$$\cos\ \theta = (\gamma_{sv}-\gamma_{sl})/\gamma_{lv}$$

Partial wetting occurs when $\gamma_{sl}<\gamma_{sv}$ (or $\theta<90°$). If γ_{sv} (or for $\theta>90°$) $\gamma_{sl}>\gamma_{sv}$, the solid will not be wetted.

The thermodynamic adhesion at the solid–liquid interface depends on the degree of interaction between both particulates of the liquid and solid. This adhesion is characterised by the work of adhesion (W_a) which is given by the Dupré's equation:[13]

$$W_a = \gamma_{lv}+\gamma_{sv}-\gamma_{sl}$$

Experimental apparatus. The apparatus employed consisted mainly of a molybdenum based resistance furnace incorporating two windows enabling the sessile drop on the substrate to be illuminated and photographed.[19] At a sufficiently slow heating rate, the level of vacuum can be maintained at 10^{-5} Pa up to a temperature of 1450 K.

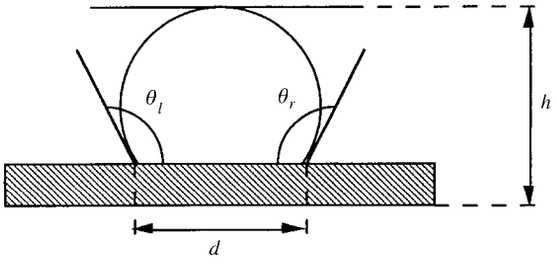

Fig. 1 Schematic representation of a liquid drop placed on a solid substrate, showing the four parameters measured as a function of time during the wettability experiments.

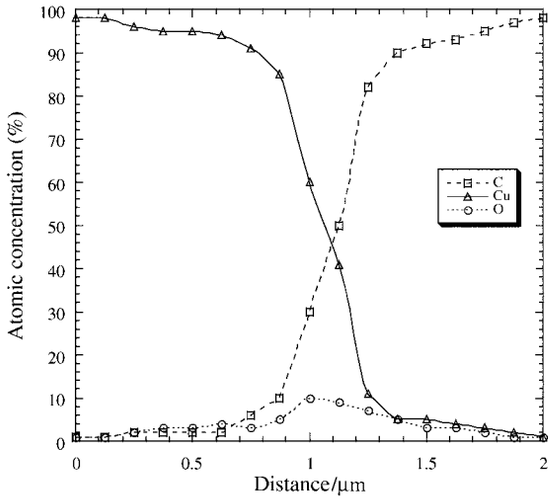

Fig. 2 AES line profile of the Cu/vitreous carbon composite across the interface.

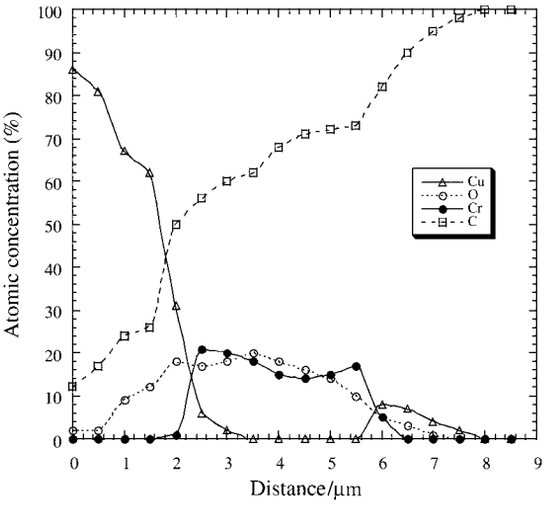

Fig. 4 AES line profile of the Cu–1 wt%Cr/vitreous carbon composite across the interface before NLLSF analysis.

3. Results

3.1 Reactivity experiments

C/Cu composite. Fig. 2 shows the AES line profile across the metal–particle interface where three regions can be observed: (i) the copper matrix, on the left side of the figure, (ii) a narrow interphase zone constituted of C and Cu in the middle section, and (iii) the carbon substrate on the right side.

C/Cu–10 wt%Sn composite. Fig. 3 shows an AES line profile across the P/M interface. The distribution of the atomic concentration of the three elements studied, tin, carbon and copper, is presented. This profile clearly shows the absence of an interfacial reaction zone. The constant tin concentration (8.52 wt%) within the matrix part is also observed. This concentration is very close to the initial matrix's composition (10 wt%).

C/Cu–1 wt%Cr composite. Figs. 4 and 5 show the distribution of the atomic concentration of the four elements studied (C, O, Cr and Cu), as a function of the distance across the M/P interface, for the original spectra and the spectra after NLLSF analysis, respectively. It can be noticed that, after the NLLSF analysis, two carbon (C–C and C–Cr), one oxygen (O–Cr) and

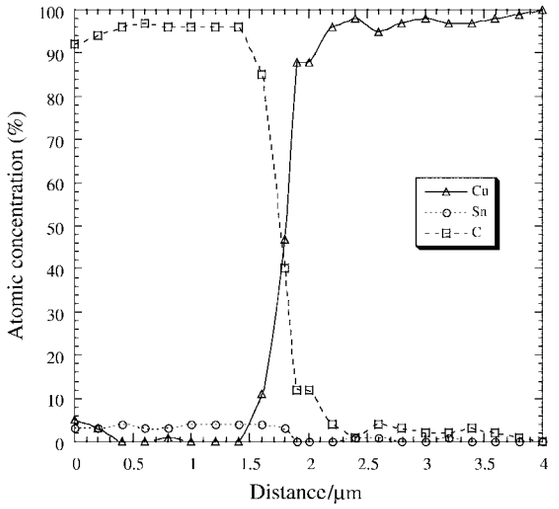

Fig. 3 AES line profile of the Cu–10 wt%Sn/vitreous carbon composite across the interface.

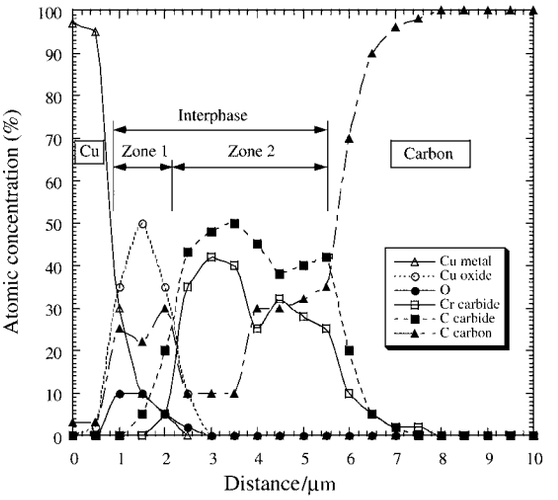

Fig. 5 AES line profile of the Cu–1 wt%Cr/vitreous carbon composite across the interface after NLLSF analysis.

two copper (Cu–Cu and Cu–O) bonds were observed. Taking these results into account Fig. 6 gives a schematic view of the qualitative chemical composition across the Cu–Cr/C interphase formed. If we do not consider the matrix and the carbon substrate, two different zones can be identified: (i) a first zone of 1 μm thickness constituted by a mixture of free carbon and copper oxide and (ii) a second zone of 4 μm thickness consisting of a more complex mixture of free carbon, chromium oxide and chromium carbide.

Electron probe microanalysis (EPMA) cartography allows

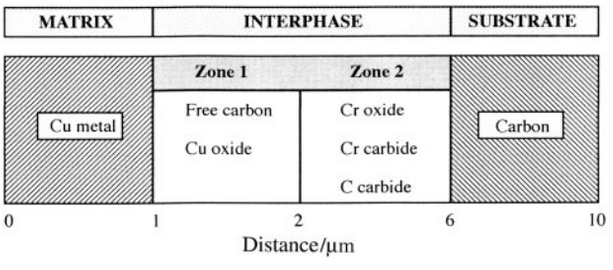

Fig. 6 Schematic representation of the chemical composition of the interphase zones developed for the Cu–1 wt%Cr/vitreous carbon composite.

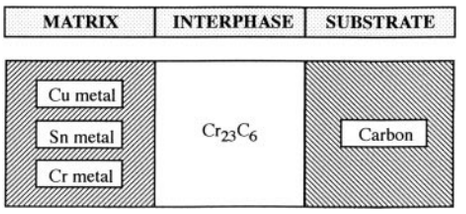

Fig. 7 Schematic representation of the interphase zones developed for a Cu–10 wt%Sn–1 wt%Cr/vitreous carbon composite.

us to confirm the segregation of the chromium alloying element preferentially at the copper alloy/graphite interface, which led to the formation of the observed chromium carbide compound.

C/Cu–10 wt%Sn–1 wt%Cr composite. The distribution of the atomic concentration of the five elements studied (C, O, Cr, Sn and C), as a function of the distance across the M/P interface, for the original spectra and the spectra after NLLSF analysis, respectively, is shown in Fig. 7. The following sequences are observed: (i) on the left side a copper–tin–chromium matrix, (ii) in the middle part an interphase zone constituted of a C–Cr carbide compound and (iii) on the right side the carbon substrate.

3.2 Wettability experiments

C/Cu composite. *Contact angle.* Values of the equilibrium contact angles θ obtained in this work, in conjunction with other reported values, are summarised in Table 1. It can be observed how the degree of graphitization of the carbon substrate and the working atmosphere are likely to influence the contact angle values, which are, in every case, close to 140°. The mode of rupture observed after cooling was of the adhesive type.

Kinetics of wettability. The kinetics of wettability of the pure copper over vitreous carbon are shown in Fig. 8. As can be observed, the drop of pure copper resting on the vitreous carbon substrate reached the equilibrium state after a very short time. These kinetics show monotonous behaviour during all of the experiments, which is mainly characterised by a constant evolution of the contact angle θ *versus* the testing time.

C/Cu–10 wt%Sn composite (see Table 1). *Contact angle.* The C/Cu–10 wt%Sn alloy exhibited a contact angle θ (46°) much smaller than that for pure copper and copper–tin systems, and a much higher work of adhesion ($W_a = 2167$ mJ m^{-2}). The mode of rupture observed after cooling was of the cohesive type.

Kinetics of wettability. The kinetics of wettability of the Cu–10 wt%Sn matrix over the vitreous carbon system presented similar characteristics to those shown by pure copper over the same substrate. It was mainly characterised by a unique stage throughout the whole of the wettability experiment, with a constant evolution of the contact angle *versus* the testing time.

C/Cu–1 wt%Cr composite (see Table 1). *Contact angle.* The C/Cu–1 wt%Cr alloy exhibited a contact angle (153°) larger than that shown for the pure copper system along with a lower work of adhesion ($W_a = 139$ mJ m^{-2}). The mode of rupture, observed after the cooling step, was of the adhesive type.

Kinetics of wettability. The kinetics of wettability obtained for the Cu–1 wt%Cr/C system, at a testing temperature of 1373 K, are presented in Fig. 9. Three different consecutive stages can be clearly identified: the first stage, which lasted for approximately the first 120 s of the wettability experiment, is characterised by a high contact angle close to 135°. A second stage occurred between 120 s and 250 s; this transition stage was characterised by a θ_1 contact angle ranging from 120° to 50°. A third stage lasted from between 250 s until the end of the experiment. At its end, a final θ_F contact angle of $46° \pm 2°$ was measured, which corresponded to an excellent wettability.

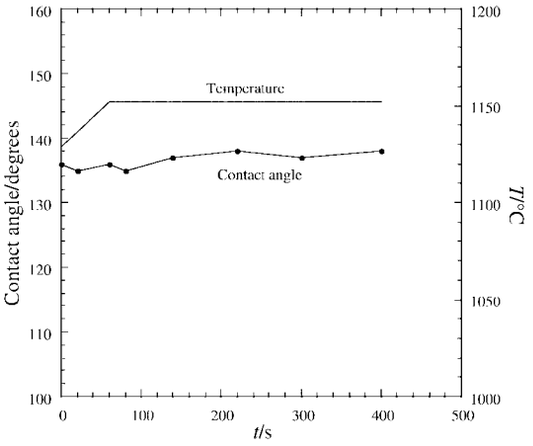

Fig. 8 Isothermal kinetics of wettability for a pure copper/vitreous carbon system at a temperature of 1423 K.

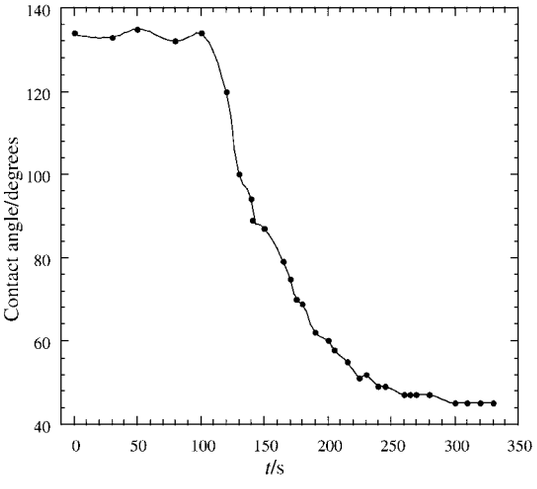

Fig. 9 Isothermal kinetics of wettability for a Cu–1 wt%Cr/vitreous carbon system at a temperature of 1373 K.

C/Cu–10 wt%Sn–1 wt%Cr composite (see Table 1). *Contact angle.* As can be seen in Table 1, a striking reduction in the contact angle (16°) (or increase in the work of adhesion) was obtained in comparison with that shown by either system. The mode of rupture observed after cooling was of the adhesive type.

Kinetics of wettability. The kinetics of wettability obtained for the Cu–10 wt%Sn–1 wt%Cr/C system, at a testing temperature of 1423 K, is presented in Fig. 10. The same three different and consecutive stages as those identified in the kinetic Cu–1 wt%Cr/C system can be clearly observed. The first stage, which lasted for the first 350 s of the wettability experiment, is characterised by a high θ contact angle close to 160°. A second stage occurred between 350 s and 2000 s; this transition stage was characterised by a θ_1 contact angle ranging from 155° to 20°. A third and final stage lasted from 2000 s until the end of the experiment. The latter stage was mainly a stationary step where the equilibrium state was reached and the θ angle only

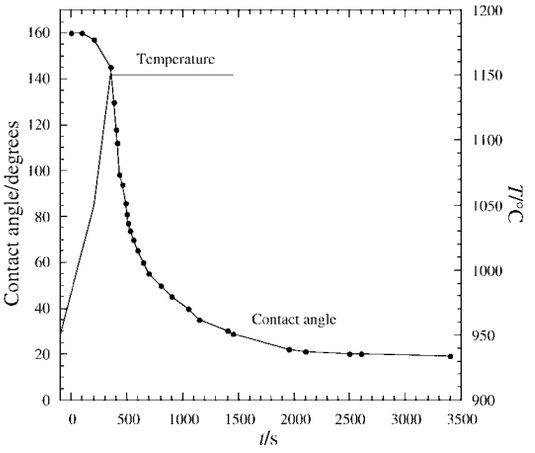

Fig. 10 Isothermal kinetics of wettability for a Cu–10 wt%Sn–1 wt%Cr/vitreous carbon system at a temperature of 1423 K.

decreased slightly with respect to the value obtained at the end of the second stage. A final θ_F angle of $16^\circ \pm 2^\circ$ was measured, which corresponds to high wettability behaviour for the system studied.

4. Discussion

Considering the results obtained, these four systems studied can be divided into two groups. The first group containing Cu/C and Cu–Sn/C, has a high contact angle ($\theta > 90^\circ$) and is characterised by adhesive solid–solid bond strengths and a monotonous behaviour during the wettability experiment. The second group containing Cu–Cr/C and Cu–Sn–Cr/C has a low contact angle ($\theta < 90^\circ$) and is characterised by cohesive solid–solid bond strengths and a complex three stage process in the wettability experiments.

4.1 Cu/C, Cu–Sn/C: physical interaction

Reactivity and contact angle. It is widely accepted that an important contribution to physical forces arises from dispersion forces. These forces, also called van der Waals interactions, arise from the interaction between an instantaneous dipole and the dipole that is induced in its vicinity. For a liquid–metal interface, the values (W_a) are usually smaller[20] than 600 mJ m^{-2}.

Taylor and Qunsheng[2] have shown that copper and copper alloys keep a constant surface tension γ_{lv} value ($\gamma_{lv1} = 1280$ mJ m^{-2}), whatever the alloying element content. The values obtained for the Cu/C ($\gamma_{lv2} = 153$ mJ m^{-2}) and Cu–Sn/C ($\gamma_{lv3} = 137$ mJ m^{-2}) systems are both much smaller than 1280 mJ m^{-2}. This large difference in surface tension values ($\gamma_{lv1} \approx 8 \times \gamma_{lv2}$ and $\gamma_{lv1} \approx 9 \times \gamma_{lv3}$) allowed us to consider the interaction between the carbon and the Cu and Cu–Sn matrices as physical interactions. For polycrystalline carbon materials, Table 1 shows that the dispersion forces are characterised by a fairly weak dependence on temperature and on the grade of graphitisation, as the different forms are very similar energetically. Indeed, because of the low values of these two γ_{lv} values, the condition of wetting, $W_a > \gamma_{lv}$, can be fulfilled only when some chemical interaction contribution complements the dispersion forces.

Kinetics of wettability. For both systems, the kinetics of wettability show a unique stage along the experiment, which is mainly characterised by a constant evolution of the θ contact angle *versus* the testing time. In non-reactive systems, such as the previous one, the kinetics are basically controlled by the viscous flow of the liquid drop over the solid substrate in the absence of any chemical interaction at the metal/substrate interface.[20,21]

4.2 Cu–Cr/C, Cu–Sn–Cr/C: chemical interaction

Reactivity and contact angle. In contrast to the non-reactive systems, the Cu–Cr/C, Cu–Sn–Cr/C systems showed W_a values greater than γ_{lv} (600 mJ m^{-2}) (see Table 2); this behaviour has been attributed to chemical interface interactions. A chemical interface interaction can be represented as resulting from a chemical reaction between a chemical species A in the liquid phase and a chemical species B in the surface of the solid to form a stable AB compound.[22]

The stability of interfaces in metal matrix composites is linked to the segregation of one of the alloy components at the metal/particle interface. This tendency of a metal to (i) segregate and (ii) wet the surface is the key problem in attempts to improve the work of adhesion.

(i) Segregation. As shown by the AES and EPMA results, Cr tends to segregate at the copper alloy/carbon interfaces. The chromium diffusion and segregation in the liquid and solid metal states and at the metal/carbon interface, respectively, may come from a different effect:

(1) During the cooling of the matrix the growth of copper grains leads to the segregation of chromium around the carbon particles.

(2) Chemical interactions between Cr atoms and C atoms may lead to Cr flux towards the carbon substrate to form a carbide compound.

(ii) Reaction induced wetting. The Cr metal can react with carbon to form carbides, thus one deals with an interface of the type liquid metal–carbide rather than liquid metal–carbon (*cf.* Fig. 11) leading to a θ contact smaller than 90° and a cohesive failure inside the metal constituent.

For the C/Cu–10 wt%Sn–1 wt%Cr system the increase in wettability, observed with respect to the C/Cu–1 wt%Cr system, can be attributed to the synergetic effect of both the chromium and tin elements. Therefore, chromium is tension active at the solid–liquid interface whereas tin is active on the free liquid surface thereby reducing the surface energy of the liquid on the copper metal.

Kinetics of wettability. Because the kinetics of wettability of the two systems are equivalent (with just time scale variation), a general discussion is proposed. As it was seen previously in the

Table 2 Wettability results obtained for the four-tested matrices/carbon systems

Alloy	T/K	$\theta_F{}^b$/°	$W_a{}^a$ /mJ m^{-2}	Mode of rupture	Interfacial reaction zone
Pure copper	1423	137 ± 5	343	Adhesive	No
Cu–10 wt%Sn	1343	153 ± 7	139	Adhesive	Yes
Cu–1 wt%Cr	1373	46 ± 2	2167	Cohesive	No
Cu–10 wt%Sn–1 wt%Cr	1423	16 ± 2	2508	Cohesive	Yes

[a]Values are calculated assuming a constant value of $\gamma_{Cu/v}$ whatever the alloying element content.[12] [b]θ_F = final contact angle.

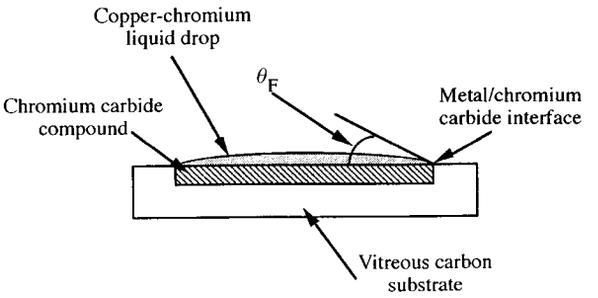

Fig. 11 Schematic view showing chromium carbide formation at the metal–substrate interface.

results section, three steps are clearly evidenced for the Cu–Cr/C and Cu–Sn–Cr/C systems. Each step is discussed separately with respect to the elaboration condition and the chemical behaviour.

Step 1: due to the residual oxygen content inside the wettability apparatus and the affinity of Cr for oxygen, the high θ_0 contact angle measured during this step was attributed to the formation of an oxide film. This oxide results from the following equation:

$$2Cr_{(Cu-Cr)} + 3/2O_2 \rightarrow 3Cr_2O_{3(\text{drop surface})}$$

This oxide film, which completely covered the surface of the liquid drop, prevents direct contact with the vitreous carbon substrate. The θ angle measured between an oxidised liquid drop on a given substrate does not depend on the nature of both the liquid and the solid substrate and is close to 140°.

On the other hand, this first step is mainly controlled by the deoxidisation of the Cu–Cr liquid drop. Two possible mechanisms can be proposed for the deoxidisation of the liquid drop: (i) formation of carbon monoxide (CO) gas, due to the presence of the vitreous carbon substrate and (ii) formation of chromium oxide. These two mechanisms result from the following equations:

$$Cr_2O_{3(\text{solid})} + 3C_{(\text{solid})} \rightarrow 3CO_{(\text{gas})} + 2Cr$$

$$Cr_2O_{3(\text{solid})} + Cr_{(\text{liquid})} \rightarrow 3CrO_{(\text{gas})}$$

From thermodynamical calculations (see for details ref. 21), it can be shown that the deoxidisation process of the oxide skin would be mainly due to the formation of carbon monoxide, the formation of chromium oxide playing a minor role in the process.

Step 2: After deoxidisation of the liquid drop, the liquid metal can react with the carbon substrate. As has been seen previously, the segregation of chromium at the M/P interface allowed chemical reaction of Cr with C to form carbide; this formation leads to a reduction in the liquid–solid interface energy (γ_{ls}). In this way the striking reduction of the θ angle value and the corresponding improvement in the wettability were due to the progressive reduction of the γ_{ls} value as a result of chromium carbide compound formation at the metal–substrate interface. Taking into account the results reported by Devicent *et al.*[12] for the same system, at a similar testing temperature, the γ_{ls} value is clearly reduced from 1975 mJ m^{-2}, for the pure copper/carbon system, to 159 mJ m^{-2} due to the presence of 1 wt% of the chromium alloying element.

Step 3: This third step was mainly a stationary step, where the equilibrium state was reached, and the θ angle only decreased slightly with respect to the value obtained at the end of the second step.

5 Conclusion

The effects of carbide alloying elements such as chromium and tin on the bonding sate and the interfacial carbon/copper zone in copper melts have been investigated. Non-wetting systems ($\theta > 90$) such as C/Cu and C/Cu–Sn are characterised by (i) an adhesive solid–solid bond strength and van der Waals interactions and (ii) monotonous behaviour during experiments where the kinetics are controlled by the viscous flow of the liquid drop over the solid substrate. Wetting systems ($\theta < 90$) such as C/Cu–Cr and C/Cu–Sn–Cr have completely different behaviour. For these two systems, chromium tends to segregate at the reinforcement–metal interface and to form stable carbide compounds. Chromium segregation and carbide formation processes lead to different kinetics of wettability that can be summarised as a 3 step process. The first step is mainly controlled by deoxidation of Cu–Cr liquid drop leading to the formation of Co and/or CrO gases. In the second step, spreading of the liquid drop is governed by an interfacial reaction process and carbide formation whereas the third and final step can be considered as a stationary step where the equilibrium state is reached.

Acknowledgements

The authors thank Dr Eustathopoulos for helpful advice and discussion.

References

1 I. G. Greenfield, *Metal and ceramic matrix composite: Proceeding, Modelling and Mechanical Behaviour*, eds. R. B. Bhagat, A. H. Clauer, P. Kumar and A. M. Ritter, The Minerals Metals and Materials Society, The Netherlands, 1990, pp. 39–46.
2 R. Taylor and Y. Qunsheng, *Proceeding of the Eight International Conference on Composite Materials (ICCM 8)*, Honolulu, 15–19 July, 1991.
3 J. F. Silvain, Y. Le Petitcorps, E. Sellier, P. Bonniau and V. Heim, *Composites*, 1994, **25**, 570.
4 A. K. Misra, *Thermodynamic Analysis of Compatibility of Several Reinforcement Materials With Beta Phase NiAl Alloys*, NASA Contractor Report 4171, Case Western Reserve University, Cleveland, Ohio, 1988.
5 J. F. Silvain, Y. Le Petitcorps, M. Layahe and M. Turner, *Surf. Sci.*, 1996, **352–354**, 839.
6 J. R. Arthur and A. Y. Cho, *Surf. Sci.*, 1973, **36**, 641.
7 D. A. Mortimer and M. Nicholas, *J. Mater. Sci.*, 1970, **51**, 49.
8 G. Grottepain, A. M. Huber, E. Borbier and G. Gillman, *Inst. Phys. Conf. Ser.*, 1986, **35**, 453.
9 R. Standing and M. Nicholas, *J. Mater. Sci.*, 1978, **13**, 33.
10 J. G. Li, *J. Mater. Sci. Lett.*, 1992, **11**, 1551.
11 Y. V. Naidich and G. A. Kolesnichenko, *Surface Phenomena in Metallurgical Processes*, ed. A. I. Belyaev, Consultants Bureau, New York, 1965, p. 218.
12 S. M. Devicent, D. L. Ellis and G. M. Michael, *Surface Phenomena in Metallurgical Processes Materials*, ed. M. D. Sacks, The American Ceramic Society, Westerville, Ohio, 1991, p. 205.
13 K. Landry, PhD thesis, Institut National Polytechnique de Grenoble, 1995.
14 J. F. Silvain, Y. Le Petitcorps and L. Albingre, *Rev. Metall. (Paris)*, 1994, **9**, 1348.
15 Y. Le Petitcorps, J. M. Poueylaud, L. Albingre, B. Berdeu, P. Lobstein and J. F. Silvain, *Key Eng. Mater.*, 1997, **127–131**, 327.
16 S. J. Sun and M. D. Zhang, *J. Mater. Sci.*, 1991, **26**, 5762.
17 L. Ramqvist, *Int. J. Powder Metall. N. Y.*, 1965, **4**, 1.
18 B. Ja. Ber, A. N. Raev and D. A. Zushinskiy, *J. Electron Spectrosc. Relat. Phenom.*, 1994, **68**, 659.
19 N. Eustathopoulos, J. C. Joud, P. Desre and J. M. Hicter, *J. Mater. Sci.*, 1974, **9**, 1233.
20 J. V. Naidich, *Prog. Surf. Membr. Sci.*, 1991, **14**, 353.
21 J. C. Bihr, PhD thesis, University Bordeaux I, France, 1997.
22 F. Delannay, L. Froyen and A. Deroyttere, *J. Mater. Sci.*, 1987, **922**, 1.